



Physico-chemical and Textural Properties of 3D Printed Plant-based and Hybrid Soft Meat Analogs

Tianxiao Wang^{1,2} · Lovedeep Kaur^{1,2} · Akashdeep Singh Beniwal^{1,2} · Yasufumi Furuhashi³ · Hiroaki Aoyama³ · Jaspreet Singh^{1,2}

Accepted: 23 April 2023 / Published online: 18 May 2023
© The Author(s) 2023

Abstract

This study investigated the physico-chemical and textural properties of 3D-printed pea protein-only and pea protein-chicken-based hybrid meat analogs. Both pea protein isolate (PPI)-only and hybrid cooked meat analogs had a similar moisture content of approximately 70%, which was similar to that of chicken mince. However, the protein content increased significantly with the amount of chicken in the hybrid paste undergoing 3D printing and cooking. Significant differences were observed in the hardness values of the non-printed cooked pastes and the 3D printed cooked counterparts, suggesting that the 3D printing process reduces the hardness of the samples and is a suitable method to produce a soft meal, and has significant potential in elderly health care. Scanning electron microscopy (SEM) revealed that adding chicken to the plant protein matrix led to better fiber formation. PPI itself was not able to form any fibers merely by 3D printing and cooking in boiling water. Protein-protein interactions were also studied through the protein solubility test, which indicated that hydrogen bonding was the major bonding that contributed to the structure formation in cooked printed meat analogs. In addition, disulfide bonding was correlated with improved fibrous structures, as observed through SEM.

Keywords Food 3D printing · Hybrid meat analogs · Texture · Microstructure · Pea protein · Chicken

Introduction

Three-dimensional (3D) printing is a novel manufacturing technology that is gaining a lot of attention for its application in the food industry. It has been used in the construction, medical, and aerospace industry utilizing diverse materials such as plastic, metal biopolymers etc. [1–4]. 3D printing creates unique geometric shapes using three-dimensional computer-aided design (CAD). Therefore, the 3D structures are built through the layer-by-layer deposition of material

inks which is fed into the 3D printers and squeezed from the nozzles of printers [4]. There are various categories of 3D printing techniques explained in detail by Tejo-Otero and team [4].

Meat analogs are generally made from vegetables or plants rich in protein and are considered a replacer by mimicking the characteristics of meat. Currently, techniques like high moisture extrusion and shear cell are used to create fibrous structures in plant protein dispersions through shear and mixing. The use of 3D printing for manufacturing meat analogs has been explored in recent years [5–7], showing the feasibility of printing products that look like meat by using plant-based materials. Currently, there is limited available literature on the characterization of 3D-printed meat analogs [8]. However, the physico-chemical properties of meat analogs after cooking were not evaluated in that study. According to previous research, textural profiles, nutrient contents, microstructure, and protein-protein interactions are major properties of meat analogs, which have been frequently measured through instruments [9–12].

Previous studies have indicated that the textural properties of 3D printed products are related to the food composition

✉ Lovedeep Kaur
L.Kaur@massey.ac.nz

✉ Jaspreet Singh
J.X.Singh@massey.ac.nz

¹ School of Food and Advanced Technology, Massey University, Palmerston North, New Zealand

² Riddet Institute, Massey University, Palmerston North, New Zealand

³ Ajinomoto Co., Inc, Suzuki-cho 3-1, Kawasaki-ku, Kawasaki-shi, Japan

and nozzle size [1, 13]. Huang et al. [13] pointed out that the 3D slicer design was changed by the nozzle size setting. A smaller nozzle diameter resulted in more layers in the sliced objective, which decreased the hardness of printed products. To produce texturally modified foods, it is significant to know how food formulation or printing performance influences food texture. Liu et al. [2] highlighted the relationship between ingredients, printing ability, and food microstructure. Their study identified that whey protein isolate helps create smooth interfaces and increased the stability of printed milk powder. Pea protein has gained a lot of popularity recently as an alternative protein source [14]. A companion paper by the authors [15] describes the detailed process of printing nugget-shaped soft meat analogs by using pea protein isolate (PPI)-only and PPI-chicken-based formulations. The addition of raw chicken paste to cooked PPI-based paste was recommended as it provides the rheological properties required for 3D printing. The main objective of the current study was to assess and compare the physico-chemical and textural properties of the printed plant-only and hybrid meat analogs.

Materials and Methods

Materials

Commercial chicken mince (5% fat and 95% protein) and beef fat (Premium 100% pure beef dripping, Farmland foods, NZ) were purchased from a local supermarket, while PPI (80% protein) was sourced from Davis Ingredient Ltd. (Palmerston North, NZ). Maize starch (pregelatinized, Hi-Maize 1043, National starch and Chemical NZ Ltd.) and soy lecithin (Hawkins Watts Ltd., NZ) were also used.

Sample Preparation and 3D Printing

Freshly prepared PPI and PPI pastes containing 20 and 50% chicken (replacing PPI, w/w) were used and are referred to as PSF, 20CHK and 50CHK, respectively. Both these pastes also contained the same amounts of added beef fat, starch and soy lecithin. The amount of water added to make the pastes was adjusted considering the moisture content of the chicken mince in order to keep the total moisture content of the pastes the same- approx. 69%. The details of the methodology to prepare the pastes are presented in detail in a companion paper [15].

An assembled LVE 3D printer (NZ-3D Ltd., New Zealand) was used (Supplementary Figure S1). More details of the printing process are provided elsewhere [15]. A 3D chicken nugget model, built using 3D builder (Version 18.0.1931.0; Microsoft Co.), was loaded and sliced

by Repetier Host (Version 2.1.4; Hot-World GmbH & Co. KG.). A small nugget shape sample was printed using the pastes at room temperature, with a printing speed of 15 mm/s and 100% infill density. The diameter of the nozzle was 1.54 mm, and the layer height was 1.5 mm. Printed samples were stored in a refrigerator overnight before transferring and sealing in polypropylene bags for cooking in a boiling water bath for 10 min.

Moisture and Protein Analysis of Printed Products

The moisture contents of the printed and cooked samples were determined by the hot air oven method [16], with minor modifications. Pre-weighed samples were dried in a hot air oven (108 °C) overnight before weighing them again to calculate their moisture content. The Kjeldahl method was used to determine the protein content [17]. A nitrogen-to-protein conversion factor of 6.25 was used for both pea and chicken protein in this study.

Textural Profile Analysis (TPA) of Printed Chicken and Printed Analogs

The texture analysis method of printed samples was inspired by Yang et al. [18], who printed samples with a simple cube shape, which was convenient for texture profile analysis. In this study, non-printed samples (including PSF, 20CHK, 50CHK, and chicken mince) were prepared in the same way as described previously. After that, 20CHK, 50CHK, and chicken mince samples were cooked in boiling water for 10 min. Finally, all of them were cut into $2 \times 2 \times 2$ cm³ cubes for further analysis. Small cubes of printed PSF, 20CHK, and 50CHK samples were prepared and cooked in the same condition as non-printed samples. Considering the printing defects and cooking shrinkage, a bigger cube size ($2.5 \times 2.5 \times 2.5$ cm³) was printed (Fig. 1). Then the bigger cubes were cut into $2 \times 2 \times 2$ cm³ after cooking. Both printed and non-printed samples were stored at 4 °C overnight and kept at room temperature for 30 min before texture analysis.

All samples were positioned on the stage of the Texture Analyser (TA.XT.plus, Stable Micro Systems, UK). The setup and calculation followed the method described by Samard and Ryu [19], with slight modifications. A 61 mm plate cylindrical probe and a load cell with a 50 kg capacity were chosen, and the measurement was based on a double compression test. Each sample was compressed twice with a 50% strain. The speed of the probe was 2 mm/s with 1 mm/s pre-test speed and 5 mm/s post-test speed. The gap time between the two compressions was 5 s. Hardness, springiness, cohesiveness, and chewiness were calculated by the software Exponent (version 6.1.16.0, Stable Micro Systems, UK).



Fig. 1 3D printed 20CHK cube

Table 1 Five extraction solutions prepared by combinations of chemicals and reagents

^{1,2} Extraction solution	Description
PB	0.1 M phosphate buffer (pH 7.5)
PS	PB + 1.5 g/100 mL SDS
PD	PB + 0.05 M DDT
PU	PB + 8 M urea
PSDU	PB + 1.5 g/100 mL SDS + 0.05 M DDT + 8 M urea

¹ PB represents phosphate buffer; PS represents PB + sodium dodecyl sulfate (SDS); PD represents PB + dithiothreitol (DTT); PU represents PB + urea; PSDU represents PB + SDS + DDT + urea. ² PB with a neutral pH was used as the control extraction solution to dissolve native protein. SDS, DTT, and urea were used to destroy hydrophobic interactions, disulfide bonding, and hydrogen bonding, respectively.

Microstructure of Chicken and Printed Meat Analogs

Both printed samples and chicken mince were placed in polypropylene bags and cooked for 10 min in boiling water. Non-printed samples were vacuum-packed, while printed samples were packed without vacuum sealing. Cooked chicken and printed meat analogs were fractured by hand. Fractured samples were pre-frozen at -30 °C overnight and then freeze-dried in a Cuddon FD18CT freeze drier (Cuddon Blenheim) at -40 °C for about 3 days. One tiny piece was taken from the fractured surface of each sample and coated with 100 nm of gold by a sputter coater (Bal-tec SCD 050) for 200 s. The microstructure of coated samples was observed and photographed by an FEI Quanta 200 Environmental scanning electrical microscope (Philips Electron Optics, USA) at 400× magnifications, with an accelerating voltage of 25 kV.

Protein Interactions (Protein Solubility Test)

Five different extraction solutions were used to dissolve different chemical bonds in the printed samples and pastes (Table 1), as described by Chiang et al. [12], with minor modifications.

Printed PSF, 20CHK, 50CHK, and non-printed raw PSF paste (0.5 g) were weighed and dissolved with 10 mL of different extraction solutions in centrifugation tubes and shaken for 30 min in a refrigerated incubator shaker. Then they were further blended with the help of a high-speed disperser (Ultra-Turrax® T25 Basic, IKA, Germany) at 4,390 × g for 30 s. and shaken again for another 30 min. Finally, samples were centrifugated in Heraeus™ Multifuge™ X3R centrifuge (Thermo Fisher Scientific, New Zealand) at 3,494 × g for 10 min. The supernatant (5 μL) of each centrifuged sample was pipetted into a microplate with 250 μL Bradford reagent (Thermo Fisher Scientific, New Zealand) and the protein amount in supernatants was measured by a microplate reader (SPECTROstar Nano, BMG Labtech, Australia) at 595 nm. The standard absorbance curve was obtained by measuring protein content in bovine serum albumin (BSA). Finally, the percentage of soluble protein was calculated:

$$\% \text{ Solubility} = \frac{\% \text{ soluble protein}}{\% \text{ total Protein}} \times 100$$

Where % total protein was measured by the Kjeldahl method [17].

Statistical Analysis

The data presented in the results and discussions are the mean values of triplicated measurements. One-way analysis of variation (ANOVA) and Tukey's pairwise comparisons were conducted by Minitab (version 18.1, Minitab Inc., State College, PA) to analyze the significance of the data. Statistical significance was defined by a *p-value* lower than 0.05.

Results and Discussion

Moisture and Protein Contents

Moisture content in PSF is lower than in samples with chicken, but there is no significant difference ($p < 0.05$, Table 2). Yao et al. [10] found that extruded meat analogs containing approximately 60% moisture showed a desirable fibrous structure that was not observed in samples with around 70% moisture. It may partly explain why the PSF

Table 2 Moisture and protein contents of the cooked 3D-printed samples

¹ Samples	^{2,3} Moisture (%)	^{2,3} Protein (%)
PSF	69.13 ± 0.40 ^a	19.19 ± 0.30 ^a
20CHK	70.45 ± 0.43 ^a	20.73 ± 0.23 ^b
50CHK	70.04 ± 0.43 ^a	22.88 ± 0.29 ^c
Chicken	70.20 ± 0.90 ^a	26.95 ± 0.48 ^d

¹PSF represents PPI paste containing both starch and fat; 20CHK represents 20% chicken added into PSF paste; 50CHK represents 50% chicken added into PSF paste. ²Results are shown as means ± SD (n = 3). ³different letters in each column show a significant difference ($p < 0.05$).

sample had little fiber formation after printing and cooking. For 3D printing, however, reducing the moisture content of PPI paste would decrease the flowability. PPI paste becomes too dry if the moisture content is reduced to 60%. On the other hand, adding other solid ingredients might cause the paste to be too sticky (According to preliminary experiments [15]).

For meat analogs, protein content is relevant to their nutritional value. In this study, protein content was higher in the sample containing a higher amount of chicken (Table 2). Protein in the boiled chicken sample was nearly 27%, which is significantly higher than in other samples ($p < 0.05$).

Texture Profile Analysis

The instrumental hardness of food products refers to the force to break food samples by molar teeth [20]. As can be seen in Table 3, all meat analog samples have a significantly lower hardness than cooked chicken mince ($p < 0.05$). The 3D printing process approximately halves the hardness of non-printed meat analogs. The hardness reduction is related to the space between deposition lines in the printing process. The restructured food material contributes a less intensive matrix compared with non-printed samples.

The hardness was reduced with the increasing amount of pea protein paste. Due to all samples containing roughly the same level of moisture, the different values of hardness should be caused by the varying formulations. As stated

by previous researchers, pea protein tends to form a soft gel [21, 22]. This could be the reason why the hardness of cooked PSF is approximately 10 times lower than cooked chicken. In addition, the hardness of 50CHK is lower than the average hardness of cooked chicken mince and PSF. The presence of protein-polysaccharides may result in the incompatibility of phases during thermal processing leading to repulsive forces causing a break in restructured PSF blend leading to reduced hardness [23].

Other textural properties, including springiness, cohesiveness, and chewiness, are listed in Table 3. These characteristics of meat analogs are also important as they are often referenced in previous research. Cooked chicken mince showed higher values than printed meat analogs. Meanwhile, these textural values of non-printed meat analogs decreased by lowering the amount of chicken. This indicates that adding chicken positively influences springiness, cohesiveness, and chewiness.

The 50CHK sample showed an increased springiness and a decreased cohesiveness after printing. It is associated with the high void rate in printed 50CHK caused by non-smooth printing behavior. In contrast, the printing process reduced springiness and improved the cohesiveness of 20CHK, which might be because of the lower void rate. As to the PSF sample, both springiness and cohesiveness were significantly changed after printing ($p < 0.05$). It might be because a pastier material such as cooked PSF paste was restructured after being extruded and deposited to form a 3D shape. While cooked pastes with chicken were less influenced post-printing due to their more solid-like nature. The chewiness values are generally related to the hardness of samples since a hard sample also exhibits a high chewiness. However, the chewiness of printed PSF is higher than non-printed PSF. In addition, printed PSF shows a huge variation in chewiness, suggesting that printed PSF should be analyzed under a lower load force.

Table 3 Textual profiles of printed and non-printed samples after cooking

¹ Samples	^{2,3} Hardness (N)	^{2,3} Springiness (%)	^{2,3} Cohesiveness (%)	^{2,3} Chewiness (N)
Chicken mince	46.99 ± 4.00 ^e	87.31 ± 2.53 ^d	48.21 ± 1.57 ^d	19.82 ± 2.36 ^d
50CHK	control	16.14 ± 1.14 ^d	72.23 ± 8.82 ^{cd}	33.55 ± 2.61 ^c
	printed	8.67 ± 0.99 ^c	85.17 ± 10.89 ^d	2.26 ± 0.34 ^{bc}
20CHK	control	7.21 ± 0.45 ^{bc}	55.10 ± 2.90 ^{bc}	24.58 ± 1.43 ^{ab}
	printed	3.46 ± 0.62 ^a	38.79 ± 6.98 ^{ab}	20.98 ± 3.12 ^a
PSF	control	4.08 ± 0.28 ^{ab}	29.95 ± 5.32 ^a	20.60 ± 0.95 ^a
	printed	1.23 ± 0.23 ^a	68.80 ± 27.2 ^{cd}	31.86 ± 9.86 ^{bc}

¹ PSF represents PPI paste containing starch and fat; 20CHK represents 20% chicken added into PSF paste; 50CHK represents 50% chicken added into PSF paste. All samples were cooked in boiling water for 10 min. ²Results were means ± SD (n = 5), obtained from Exponent. ³different letters in each column show a significant difference ($p < 0.05$).

Microstructure of Cooked Chicken and Printed Meat Analogs

The photos of printed uncooked and cooked meat analogs are shown elsewhere [15]. The PSF was inadequate to form a fibrous structure. More fibers were found in the cooked 20CHK than 50CHK sample. It might be because of a smoother printing flow of 20CHK. Printed PSF showed a highly aggregated microstructure with globular particles

inside (Fig. 2). The aggregation is assumed to consist of PPI, starch, and fat. Feng et al. [24] found similar aggregation constructed by a starch and pea protein network through SEM. Although starch was the major ingredient in their study, they demonstrated that an increasing amount of pea protein began to establish a continuous pea protein matrix. The 20CHK sample exhibits a layered structure, but no fibrous structure was observed. The visible aligned fibrous structure in the 50CHK was observed inside the

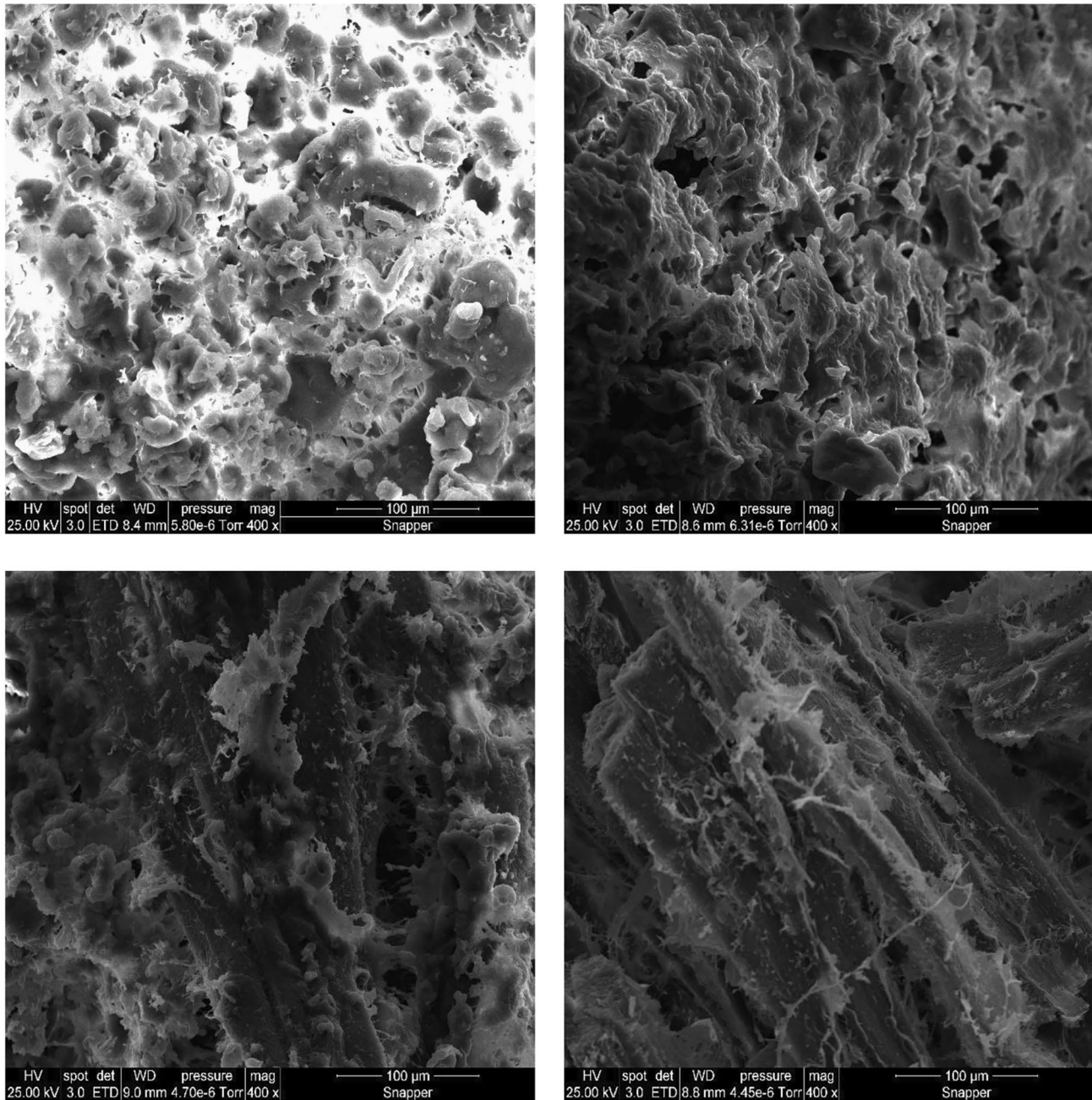


Fig. 2 Microstructure of cooked printed meat analogs (PSF (top left), 20CHK (top right), 50CHK (lower left)) and non-printed chicken mince (lower right) viewed by SEM at 400×magnification

PSF represents PPI paste containing starch and fat; 20CHK and 50CHK represent 20 and 50% chicken added into PSF paste.

plant protein-based matrices (Fig. 2). A similar fibrous structure is also found in cooked chicken mince. The structure of cooked chicken mince was very similar to chicken meat under SEM in previous studies [13, 19]. It indicates that cooked chicken mince exhibits fibers.

These findings suggest that the fibrous structure is created by chicken directly. PPI or other ingredients would not provide fiber through the preparation and printing process in this study. The large proportion of chicken paste in the 50CHK samples assists in forming obvious fibers. However, such structure also negatively influenced the extrusion smoothness, resulting in poor printing performance with few fibers presented in the macrostructure [15]. To print a fibrous non-meat product, other potential plant-based fiber-forming agents need to be added. More research on fiber-forming mechanisms is required.

Protein Solubility

Protein solubility was found to be the lowest in PB compared with all extraction solutions (Fig. 3). It indicates that protein interactions exist and supports the structure of samples. Even though the PSF paste showed a significantly higher solubility than the other three samples in PB ($p < 0.05$), it was still lower than 5%. Such low solubility further proves that the PPI used in this study had already been denatured during the manufacturing process since only native plant protein can be dissolved in a phosphate buffer [9]. It was obvious that soluble protein in PU was higher than in PS and PD, demonstrating that proteins are more

soluble in urea than in SDS and DTT. It is believed that urea destroys hydrogen bonds [25]. Thus, hydrogen bonding is considered the major interaction between proteins in all samples. Previous research also showed that hydrogen bonds were the major force in pea legume protein gel [26].

Protein-protein interactions have been recognized as a mechanism of fiber formation. The formation of fibrous structures is associated with the formation of hydrophobic interactions, disulfide bonds among proteins, or the combination of both bonds [27]. Extruded meat analogs tended to show a high protein solubility in DTT solvents, as it breaks disulfide bonding [9, 13]. In this study, the disulfide bond is also considered as the main protein-protein interaction responsible for fibrous structures. This is because chicken-added samples, which have a fibrous structure, showed lower protein solubility in overall extraction solutions except in DDT-containing buffer solution (PD). However, PSF paste and printed PSF did not show significantly different ($p < 0.05$) protein solubility in PD, interpreted as showing that printing and cooking did not help form fibers. It has already been discussed that fibers in printed samples were mainly provided by chicken paste. Similar to the results observed by Chiang et al. [12], the protein solubility of all samples in PSDU is greater than the sum of solubility in PS, PD, and PU. It indicates that the structure of PSF paste and printed meat analogs are not only supported by hydrophobic interactions, disulfide, and hydrogen bonds but also their combinations.

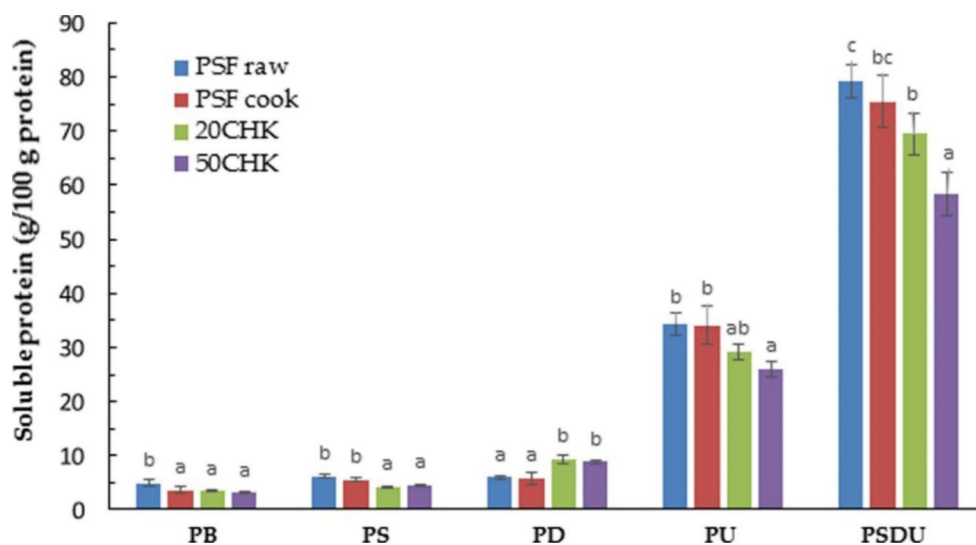


Fig. 3 Soluble protein percentages in PSF paste, Printed PSF, 20CHK and 50CHK in five extraction solutions. Each bar shows means \pm SD ($n = 3$). Data with different letters for each extraction treatment are significantly different ($p < 0.05$). PSF raw represents PPI paste containing starch and fat without cooking; Printed PSF represents PPI containing starch and fat after cooking; 20CHK

represents 20% chicken added into PSF paste; 50CHK represents 50% chicken added into PSF paste. PSF cook, 20CHK, and 50CHK samples were printed and cooked in boiling water for 10 min. PB represents phosphate buffer; PS represents PB + SDS; PD represents PB + DTT; PU represents PB + urea; PSDU represents PB + SDS + DTT + urea.

Conclusions

The meat-like fibrous structure was not clearly observed in the PPI-only sample. It is recognized that fibers in printed hybrid meat analogs are contributed by native chicken muscle fibers. Nevertheless, adding a higher amount of chicken (50CHK) decreased the extrudability, which also negatively influenced the printing performance, resulting in fewer fibers shown in the macrostructure. Through the protein solubility assay, it was known that hydrogen bonding is the major protein interaction that helps support the structure of printed meat analogs. The disulfide bonding was observed to be the main interaction related to fibrous structure. Printed meat analogs showed a higher softness compared with conventionally cooked chicken meat.

For this purpose, it is highly recommended to conduct sensory studies on 3D-printed meat analogues. People with mastication issues or who are interested in soft foods could be selected and trained as sensory panellists.

Supplementary Information The online version contains supplementary material available at <https://doi.org/10.1007/s11130-023-01068-4>.

Acknowledgements The authors acknowledge the Ajinomoto (Japan) Innovation Alliance Program and the School of Food & Advanced Technology, Massey University (NZ) for financial support.

Author Contribution T. Wang: Data analysis, Investigation, Methodology, Validation, Visualization, Writing – original draft, Writing – review & editing. Jaspreet Singh: Conceptualization, Data curation, Formal analysis, Investigation, Methodology, Software, Visualization, Writing, Funding acquisition– review & editing. Lovedeep Kaur: Conceptualization, Investigation, Methodology, Software, Visualization, Writing, Funding acquisition – review & editing. Writing – review & editing. Akashdeep Singh Beniwal: Writing – review & editing. Yasufumi Furuhashi and Hiroaki Aoyama: Methodology, Writing – review & editing. Funding: The authors J. Singh and L. Kaur have received partial funding for the work from Ajinomoto Co. Inc. (Japan). The author T. Wang was the Masters student in the project.

Funding Open Access funding enabled and organized by CAUL and its Member Institutions

Data Availability The data may be made available upon request.

Declarations

Ethics approval This article contains no studies on human or animal objects.

Consent to participate Not applicable.

Consent for publication Not applicable.

Conflict of Interest The authors J Singh and L Kaur have received

some research support for the work from Ajinomoto (Japan). Other authors have no conflict of interest to declare.

Open Access This article is licensed under a Creative Commons Attribution 4.0 International License, which permits use, sharing, adaptation, distribution and reproduction in any medium or format, as long as you give appropriate credit to the original author(s) and the source, provide a link to the Creative Commons licence, and indicate if changes were made. The images or other third party material in this article are included in the article's Creative Commons licence, unless indicated otherwise in a credit line to the material. If material is not included in the article's Creative Commons licence and your intended use is not permitted by statutory regulation or exceeds the permitted use, you will need to obtain permission directly from the copyright holder. To view a copy of this licence, visit <http://creativecommons.org/licenses/by/4.0/>.

References

1. Yang F, Zhang M, Prakash S, Liu Y (2018) Physical properties of 3D printed baking dough as affected by different compositions. *Inn Food Sci Emerg Technol* 49:202–210
2. Liu Y, Liu D, Wei G, Ma Y, Bhandari B, Zhou P (2018) 3D printed milk protein food simulant: improving the printing performance of milk protein concentration by incorporating whey protein isolate. *Inn Food Sci Emerg Technol* 49:116–126
3. Wang L, Zhang M, Bhandari B, Yang C (2018) Investigation on fish surimi gel as promising food material for 3D printing. *J Food Eng* 220:101–108
4. Tejo-Otero A, Buj-Corral I, Fenollosa-Artés F (2020) 3D printing in medicine for preoperative surgical planning: a review. *Annal biomed eng* 48(2):536–555
5. Hitti N (2018) Novameat develops 3D-printed vegan steak from plant-based proteins. <https://www.dezeen.com>. Accessed 29 December 2021
6. NOVAMEAT. Plant-Based Meat | NOVAMEAT | Barcelona <https://www.novameat.com>. Accessed 29 December 2021
7. SavorEat Ltd. More than just a meat alternative. A game-changing platform. <https://savoreat.com>. Accessed 29 December 2021
8. Shahbazi M, Jäger H, Chen J, Ettlalaie R (2021) Construction of 3D printed Reduced-Fat Meat Analog by Emulsion Gels. Part II: Printing Performance, Thermal, Tribological, and dynamic sensory characterization of printed objects. *Food Hydr* 121:107054
9. Lin S, Huff HE, Hsieh F (2000) Texture and chemical characteristics of soy protein meat Analog Extruded at High Moisture. *J Food Sci* 65(2):264–269
10. Liu K, Hsieh F-H (2008) Protein–protein interactions during high-moisture extrusion for fibrous meat analogs and comparison of protein solubility methods using different Solvent Systems. *J Agric Food Chem* 56(8):2681–2687
11. Dekkers BL, van der Nikiforidis CV (2016) Shear-Induced Fibrous structure formation from a Pectin/SPI blend. *Innovative Food Science & Emerging Technologies* 36:193–200. <https://doi.org/10.1016/j.ifset.2016.07.003>
12. Chiang JH, Loveday SM, Hardacre AK, Parker ME (2019) Effects of soy protein to wheat gluten ratio on the Physicochemical Properties of Extruded Meat Analogs. *Food Struc* 19:100102. <https://doi.org/10.1016/j.foostr.2018.11.002>
13. Huang M, Zhang M, Bhandari B (2019) Assessing the 3D Printing Precision and Texture Properties of Brown Rice Induced by Infill levels and Printing variables. *Food Bioprocess Technol* 12(7):1185–1196. <https://doi.org/10.1007/s11947-019-02287-x>

14. Qi M, Zhang G, Ren Z et al (2021) Impact of Extrusion temperature on in Vitro Digestibility and Pasting Properties of pea flour. *Plant Foods Hum Nutr* 76:26–30
15. Wang T, Kaur L, Furuhashi Y, Aoyama H, Singh J (2022) 3D Printing of Textured Soft Hybrid Meat Analogs. *Foods* 11(3):478
16. AOAC Official Methods of Analysis of AOAC International (18th ed.). AOAC, Gaithersburg, MD, USA
17. AOAC Nitrogen in meat (928.08) AOAC Official Method. <http://www.eoma.aoac.org/methods/info.asp?ID=16468>. Accessed 29 December 2021
18. Yang F, Zhang M, Bhandari B, Liu Y (2022) Investigation on Lemon Juice Gel as Food Material for 3D Printing and optimization of Printing Parameters. *LWT* 87:67–76
19. Samard S, Ryu GA (2019) Comparison of physicochemical characteristics, texture, and structure of Meat Analog and meats. *J Sci Food Agric* 99(6):2708–2715
20. Lyon CE, Lyon BG, Davis CE, Townsend WE (1980) Texture Profile Analysis of Patties made from mixed and Flake-Cut mechanically deboned Poultry Meat. *Poult Sci* 59(1):69–76. <https://doi.org/10.3382/ps.0590069>
21. Osen R, Toelstede S, Wild F, Eisner P, Schweiggert-Weisz U (2014) High moisture extrusion cooking of pea protein isolates: raw material characteristics, extruder responses, and Texture Properties. *J Food Eng* 127:67–74
22. Schreuders FKG, Dekkers BL, Bodnár I, Erni P, van der Boom RM (2019) Comparing structuring potential of pea and soy protein with Gluten for Meat Analog Preparation. *J Food Eng* 261:32–39. <https://doi.org/10.1016/j.jfoodeng.2019.04.022>
23. Dekkers BL, Hamoen R, van der Boom RM (2018) Understanding fiber formation in a concentrated soy protein isolate-pectin blend. *J Food Eng* 222:84–92
24. Chuanxing F, Qi W, Hui L, Quancheng Z, Wang M (2018) Effects of pea protein on the Properties of Potato Starch-Based 3D Printing materials. *Int J Food Eng* 14(3)
25. Uruakpa FO, Arntfield SD (2006) Impact of Urea on the microstructure of Commercial Canola Protein–Carrageenan Network: A Research note. *Int J Biol Mac* 38(2):115–119
26. O’Kane FE, Happe RP, Vereijken JM, Gruppen H, van Boekel MA, J. S (2004) Heat-Induced gelation of pea legumin: comparison with soybean glycinin. *J Agric Food Chem* 52(16):5071–5078. <https://doi.org/10.1021/jf035215h>
27. Dekkers BL, van der Boom RM (2018) Structuring processes for meat analogs. *Trends Food Sci Technol* 81:25–36

Publisher’s Note Springer Nature remains neutral with regard to jurisdictional claims in published maps and institutional affiliations.

Springer Nature or its licensor (e.g. a society or other partner) holds exclusive rights to this article under a publishing agreement with the author(s) or other rightsholder(s); author self-archiving of the accepted manuscript version of this article is solely governed by the terms of such publishing agreement and applicable law.